RESPONSE SURFACE HISTORICAL METHOD, SIMULATION OF CO_2 ABSORPTION PROCESS BY DEA IN FFR USING COMSOL MULTIPHYSICS

Nasser MALEKI,[a] Sorosh ZARINABADI,[b,*] Alireza AZIMI[a] Amirhossein Shahbazi KOOTENAEI[a]

[a]Department of Chemical Engineering, Mahshahr Branch, Islamic Azad University, Mahshahr, Iran
[b]Department of Technical and Engineering, Ahvaz Branch, Islamic Azad University, Ahvaz, Iran

Absorption of carbon dioxide as a greenhouse gas from a mixture of CO_2 and N_2 in a continuous falling film reactor (FFR) has been designed and developed. The reactor length and inner diameter were 1m and 0.021m, respectively. In this paper, the absorption of CO_2 by DEA (Diethanolamine) in FFR is studied by means of COMSOL Multiphysics and Design expert. Design expert is used to developing an empirical equation for CO_2 absorption when reacting with DEA. The simulation is performed with COMSOL Multiphysics for a second-order reaction and the velocity profile is considered the effect of shear stress. The result shows that the penetration depth of CO_2 in the falling film reactor is 0.006mm and the absorption rate increases with increasing gas flow velocity and inlet CO_2 concentration. Also, this study is performed on low Reynolds number ($1 \leq Re_G \leq 6$ and $4 \leq Re_L \leq 40$ at 298 K) which has not been considered by other researchers.
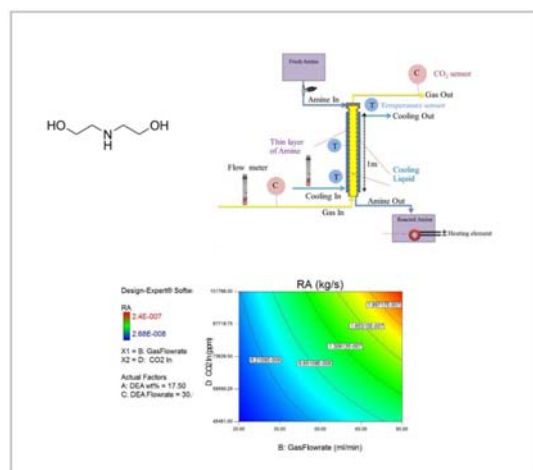
INTRODUCTION

"The ultimate objective determined by the United Nations Framework Convention on Climate Change (UNFCCC) is to achieve stabilization of greenhouse gas concentrations in the atmosphere at a level that would prevent dangerous anthropogenic interference with the climate system".[1] Therefore, reducing greenhouse gases such as CO_2 is of significant interest from an environmental point of view.[1,2]

To reduce CO_2 emission from various sources, chemical absorption has been used. Chemical absorption of CO_2 is considered as a process where CO_2 is absorbed by a liquid phase that contained reaction and absorptive mass transport. Aqueous amine solvents absorb CO_2 by chemical reaction.

These amines are classified as primary, secondary and tertiary. The reactivity order of amine to CO_2; primary>secondary>ternary. DEA (Diethanolamine) aqueous solution is a secondary amine-based system that is used to sweeten sour gas and chemical absorption of CO_2 from flue gases.[3]

Chemical absorption needed gas-liquid contact that can be achieved in a falling film reactor (FFR) or contactor. No compression is needed before feeding it into an FFR, so it can be used to absorb CO_2 from flue gases.[4]

Numerous effort has been done to predicate the mass transfer process and obtaining knowledge of the absorption process for an FFR.[5–19] The mass transfer rates are investigated for the wavy and smooth falling film. The investigation has shown

* Corresponding author: soroushzarinabadi@iauahvaz.ac.ir

that the mass transfer rate was bigger for the wavy film and mass transfer characteristics varied substantially with the wave regime.[6–9] The film hydrodynamics, such as the velocity distributions and the vorticity variations at different positions of the wavy falling films, have been enhanced the mass transfer process.[10]

The analytical and numerical model has been applied to model FFR[6-12] and FFR could be simulated by means of COMSOL Multiphysics.[13,14]

Generally, the two-film theory is used to describe gas absorption. In this theory, two resistances have existed to the CO_2 diffusion into an amine solution. First, a stagnant film existed in the gas phase and the second another stagnant film can be considered in the liquid phase. Absorption can be calculated using the mass transfer coefficient, the mass, and heat transfer conversation equation. Since solving the coupled equations are very complex and some assumption is needed to do so, the results are not very accurate.[16,17]

Since little data are available for CO_2 absorption by means of DEA using FFR, in this paper, DEA is used to absorb CO_2 from the gaseous mixture (CO_2 and N_2) and the operating parameters of FFR are investigated. Also, the absorption process in FFR for low Reynolds numbers, has been investigated and simulated using COMSOL Multiphysics. Finally, using the statistical method (Response Surface Historical Method (RSHM)) and the laboratory results, an empirical equation has been developed that could calculate CO_2 absorption.

To investigate the absorption of the flue gases from the 200-MW boiler firing low-S fuel oil, CO_2 concentration was 5% and 10%. Predicated gaseous emission of CO_2 from the 200-MW boiler firing low-S fuel oil is about 10%.[20]

MATERIALS AND METHODS

1. Materials

CO_2 and N_2 were procured from Fanavaran Petrochemical CO. Iran. DEA for CO_2 absorption was procured from Merck Company.

2. Procedure

The schematic diagram of the experimental setup and coordinate system are shown in Figure 1 and Figure 2. The setup is designed as a falling film reactor. The inner diameter of the reactor was 0.021m and the length of 1m. The flow in the reactor was counter current. The aqueous amine flowed from the reactor top. CO_2 gas was diluted to the desired concentration with nitrogen in a mixing chamber before entering the reactor from the bottom.
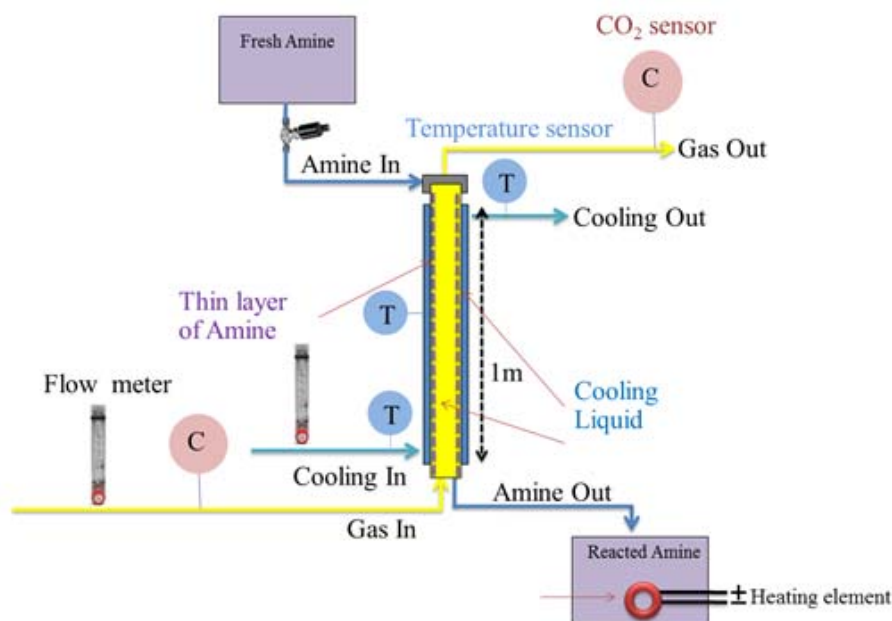
Fig. 1 – Experimental setup.
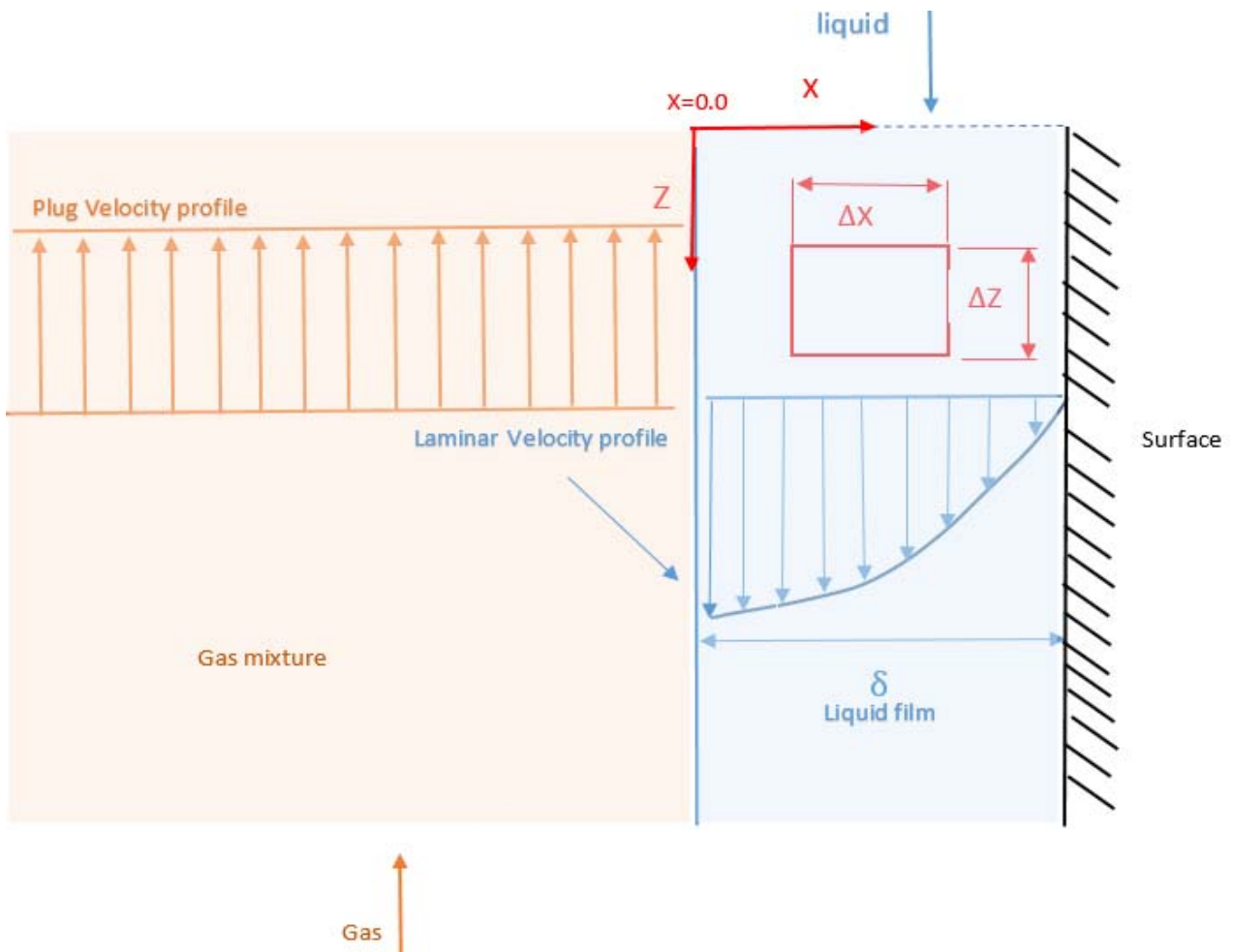
Fig. 2 – Flow model of the falling film reactor(x and z coordinate are in mm).
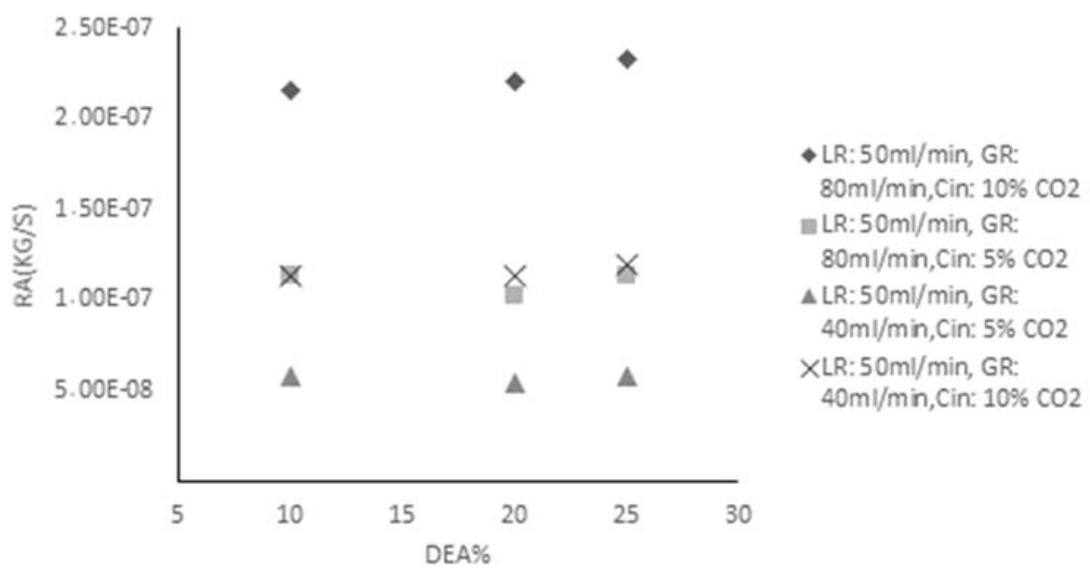
Fig. 3 – Comparison of gas absorption rate (R_A) with DEA%.
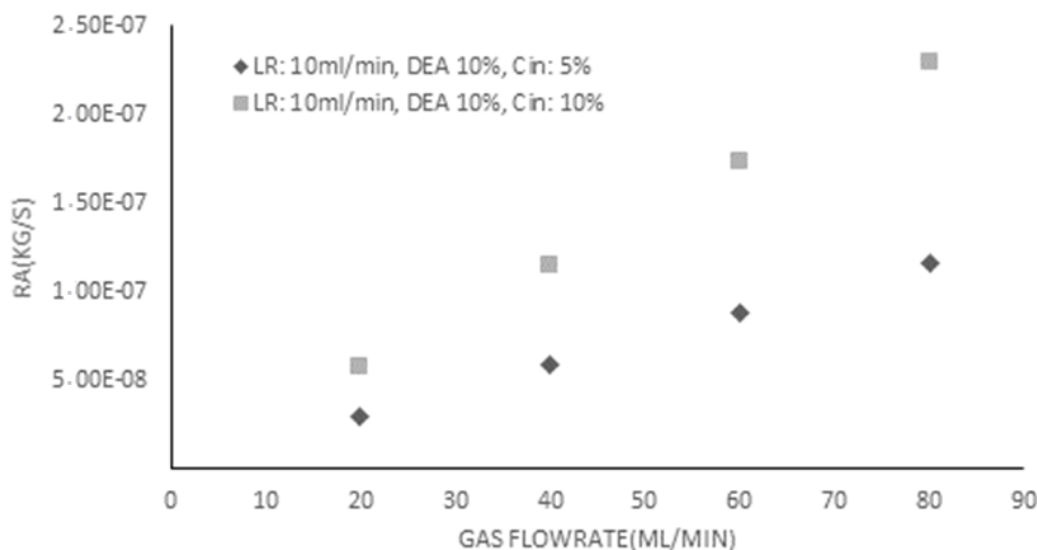
Fig. 4 – Comparison of gas absorption rate (R_A) and a gas flow rate.

All the experiments were performed at a 298K temperature and 1atm pressure. The absorbent (DEA solution) selectively absorbs CO_2 gas from the feed gas mixture and reacts simultaneously to form a stable carbamate in the reactor section. The input and output concentration of the gas were determined using two *K33 ICB 30% CO_2 Sensor* from CO_2 Meter Company. The CO_2 content can be monitored by GasLab[TM] software online. The mass rate of absorption was calculated using the following equation:

$$R_A = C_{in}Q_{Gas} - C_{out}Q_{Gas} \quad (1)$$

where C_{in} and C_{out} were input and output concentration of CO_2 to FFR respectively.

RESULTS AND DISCUSSION

The input and output ppm of CO_2 at the bottom and the top of FFR during the execution of 62 runs are tabulated in Table 1. According to the data, it is observed that with increasing amine concentration, CO_2 concentration decreases. This is because as amine concentration increases, falling film thickness also increases (see Figure 5) and as a result driving force for mass transfer increases [4]. It is obvious that increasing the gas flow rate, causing an increase in CO_2 output concentration. The absorption rate is increased slightly by increasing DEA percent (see Figure 3) but it is increased with increasing input gas flow rate and CO_2 percent (see Figure 4). This is because there is

an increase in gas Reynolds number due to increasing gas flow rate.

1. Model reaction

1.1. Physical properties of DEA

Density and viscosity of DEA solution were estimated from the work of Arachchige *et al.*[21] and Han *et al.*[22] The effect of DEA concentration and temperature on density and viscosity was considered in their experiments. The heat capacity of DEA solution was estimated from the work of Shokouhi *et al.*[23]

The diffusivity of DEA in DEA solution was estimated by the following equation:[24]

$$\ln(D) = -13.268 - 2287.7/T - 19.699 \times 10^{-5}C$$

$$\text{For } 9 \geq C \ (mol/m^3) \geq 4013 \quad (2)$$

$$298 \geq T \ (K) \geq 348$$

The diffusion coefficient of CO_2 in DEA solution and Henry's constant was estimated from the work of Abu-Arabi *et al.*[25] In the model, the thermal conductivity of the DEA solution and the heat transfer coefficient are equal to 0.4893 (W/m K) and 900(J/m^{2} s) respectively.

1.2. Physicochemical properties of CO_2

The physicochemical properties of CO_2 and the experimental conditions of the system required for the model are given in Table 2.

Table 1

Data from Lab work

Run	DEA%	Gas Rate (mL/min)	Amine Rate (mL/min)	Input CO2 (ppm)	Output CO2 (ppm)
1	10	20	10	49194	174
2	10	40	10	49570	347
3	10	60	10	49677	464
4	10	80	10	49532	819
9	10	40	50	50021	1550
10	10	80	50	50293	2769
11	10	60	50	50196	2139
12	10	20	50	50062	798
20	20	20	10	45303	182
21	25	40	10	49649	55
22	25	60	10	49803	23
23	25	80	10	49278	65
24	25	20	10	49019	30
33	10	80	10	98101	1903
34	10	80	20	98044	3559
35	10	40	20	97964	1952
42	10	60	10	98333	1119
43	20	40	20	98067	1117
44	20	80	20	98217	3239
45	20	80	50	98181	5557
46	20	40	50	97690	2118
47	20	40	10	97522	339
53	25	80	10	101355	267
54	25	20	10	100892	174
55	25	20	20	100770	316
61	25	40	50	101798	1686
62	25	20	50	101678	1146

Table 2

Experimental parameters and physiochemical properties of CO_2-DEA system

Temperature (K)	**298**
Pressure (atm)	1
Height of the column, L (m)	1
The inner diameter of the column, d (m)	0.021
Gas flow rate, Q_G (m^3/s)	3.33×10^{-7}-1.33×10^{-6}
Liquid flow rate, Q_L (m^3/s)	1.67×10^{-7}-8.33×10^{-7}
Diffusivity of CO_2 in gas, D_G (m^2/s)[4]	1.67×10^{-5}
Viscosity of gas mixture, μ_G (kg/m.s)[4]	1.72×10^{-5}
Heat of reaction (kJ/kmol)[26]	57200
Heat of solution (kJ/kmol)[26]	13240

1.3. CO_2/DEA system: reaction kinetics

The overall reaction which accounts for the reaction between CO_2 and DEA is

$$CO_2 + 2RR'NH \overset{k}{\leftrightarrow} RR'NH_2^+ + RR'NHCOO^- \quad (3)$$

The rate of the above equation can be described as:

$$r_{co_2} = -kC_{CO_2}C_{DEA} \quad (4)$$

and the second-order rate constant of the overall reaction between CO_2 and DEA was determined by:[27]

$$\text{Ln } k \left(\frac{m^3}{\text{kmol·sec}} \right) = 24 \cdot 515 - \frac{5411 \cdot 3}{T} \quad (5)$$

The following correlation is used to calculate the mass transfer coefficient for gas (k_G):

$$Sh_G = 0.02922 \, Re_G^{0.7151} Sc_G^{0.5} \quad (6)$$

This correlation is based on 62 data points and predicts the experimental data with R^2 of 0.97. The coefficients of Eq (6) are estimated using non-linear least square regression in Excel by fitting the expression to the experimental data. The correlation was valid for $1 \leq Re_G \leq 6$ and $4 \leq Re_L \leq 40$ at 298K. The gas side mass transfer coefficient depended on the gas flow rate and its properties.

In the simulation, because of the calculated Hatta number, it was assumed that the reaction between

CO_2 and DEA was instantaneous, and interpretation for the kinetic regime was performed based on the published literature for an instantaneous chemical reaction.[27] The Hatta number in the present study, is greater than 3 for a film thickness of 0.2 mm and in the fast reaction region, indicating that the reaction can be assumed as an instantaneous reaction. Based on this, and due to the high solubility of CO_2 in DEA solution, the liquid-phase mass transfer resistance was neglected.

1.4. Model equation

The following table shows the model equation.

1.5. Solution procedure and Output

To create a 2D falling film model in COMSOL Multiphysics 5.1 environment, Transport of Diluted Species (tds), Heat Transfer in Fluids (ht), Coefficient Form Boundary PDE are required. After creating the model, the parameters and boundary conditions are defined for each physics. Then, a stationary study is used to solve the coupled equations (see Table 3).

The numerical solution must be applied to the coupled equations. In the numerical solution, predefined distribution type mesh is used (Distribution 1 in x-direction: Number of element 200 and Element ratio 0.01. Distribution 2 in z-direction: Number of element 50 and Element ratio 0.01)**.** Therefore, memory and calculation time could be optimized. The film thickness of amine in the reactor was estimated by performing momentum balance in the liquid phase.[4] Figure 5 shows the film thickness and velocity profile for DEA solution. A more viscous DEA solution presents a lower velocity value at the interface and higher film thickness. "This behavior can be explained by Nusselt theory, which predicts lower velocity values and thicker liquid films as the viscosity increases".[28]

Finite element method and Non-linear solver is used to solve the non-symmetric matrix and the results are showed in the following figures. Figure 6 shows the concentration variation of CO_2 in the falling film of DEA.

Table 3

Mathematical model[4]

Chemical equation:

$$A(G) + bB(L) \rightarrow \text{Product} \tag{7}$$

Equations
Liquid Phase:

$$u_L = \frac{g}{2v_L}\delta^2\left(1 - \left(\frac{x}{2}\right)^2\right) - \frac{\tau_G\delta}{\mu_L}\left(1 - \left(\frac{x}{2}\right)\right) \quad \tau_G = f\rho_G u_G^2 \tag{8}$$

Mass Balance
Component A

$$u_L\frac{\partial C_A}{\partial z} = \frac{\partial}{\partial x}\left[D_A\frac{\partial C_A}{\partial x}\right] - kC_AC_B \tag{9}$$

Component B

$$u_L\frac{\partial C_B}{\partial z} = \frac{\partial}{\partial x}\left[D_B\frac{\partial C_B}{\partial x}\right] - kbC_AC_B \tag{10}$$

Heat Balance

$$u_L\frac{\partial T}{\partial z} = \frac{\partial}{\partial x}\left[\alpha\frac{\partial T}{\partial x}\right] + \frac{\Delta H_R}{\rho c_p}kC_AC_B \tag{11}$$

Gas-Phase:
Mass Balance
Component A

$$\frac{dw_G C_{AG}}{dz} = k_G(C_{AG} - H_0C_A) \tag{12}$$

Heat Balance

$$\frac{dw_G c_G T_G}{dz} = h_G(T_{x=0} - T_G) \tag{13}$$

Boundary Conditions
Liquid Phase:

$$\text{At } x = \delta: \qquad \frac{\partial c_A}{\partial x} = 0 \quad \frac{\partial c_B}{\partial x} = 0 \quad -k_\lambda \frac{\partial T}{\partial x} = U(T_{x=0} - T_R) \qquad (14)$$

$$\text{At } x=0: \; k_G(C_{AG} - C_A H_0) = -D_A \frac{\partial c_A}{\partial x} \quad \frac{\partial c_B}{\partial x} = 0 \quad h_G(T - T_G) - k_\lambda \frac{\partial T}{\partial x} = (-\Delta H_s) D_A \frac{\partial c_A}{\partial x} \qquad (15)$$

$$\text{At } z = 0: \; C_A = 0 \quad C_B = C_B^0 \qquad T = T_0 \qquad (16)$$

Also, Figure 7 shows the concentration variation of CO_2 in the falling film of DEA at various height (z) of the reactor (Amine flowrate: $8.33 \times 10^{-7} m^3/s$, CO_2 concentration at the input gas: 10%, DEA aqueous solution Concentration: 25% – zoom mode). The reaction of CO_2 with amine occurred in a very small section of the falling film thickness (0.006mm). The driving force of mass transfer at the bottom of the reactor is greater so the slope change is also large.

Simulation results show that the lowest concentration of DEA was $2400 mol/m^3$ so many moles of the DEA didn't react with CO_2 and could be reused. The highest concentration of CO_2 in DEA was $0.24 \ mol/m^3$ at the interface.
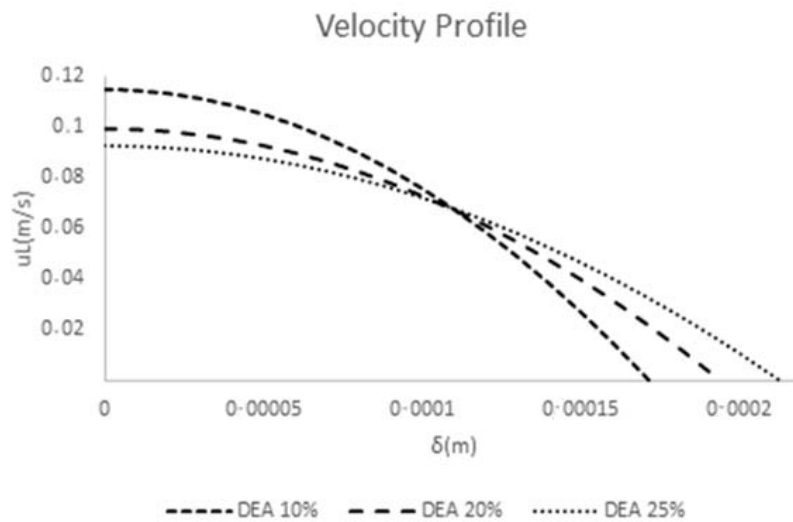
Fig. 5 – DEA velocity profile with various concentration, DEA flow rate: 8.3×10^{-7} Gas flow rate: 6.7×10^{-7}.
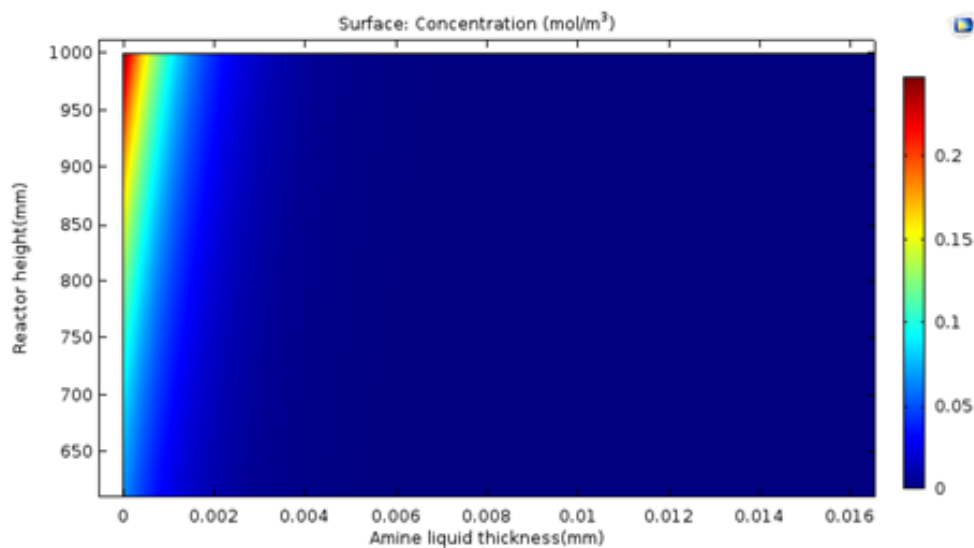
Fig. 6 – Liquid concentration of CO_2 in the falling film reactor in zoom condition.
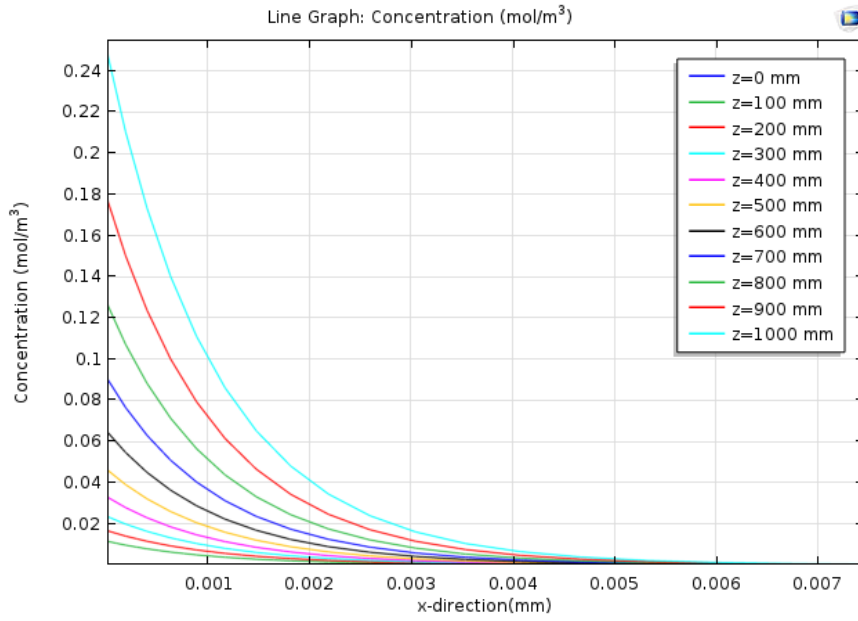
Fig. 7 – CO_2 Concentration in DEA at the various height of the reactor.
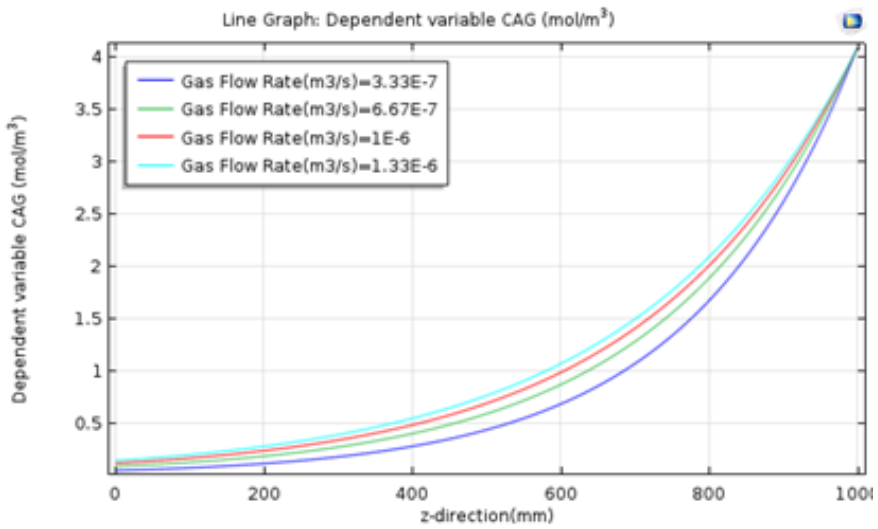
Fig. 8 – CO_2 Concentration for various gas flow rate in the gas phase.
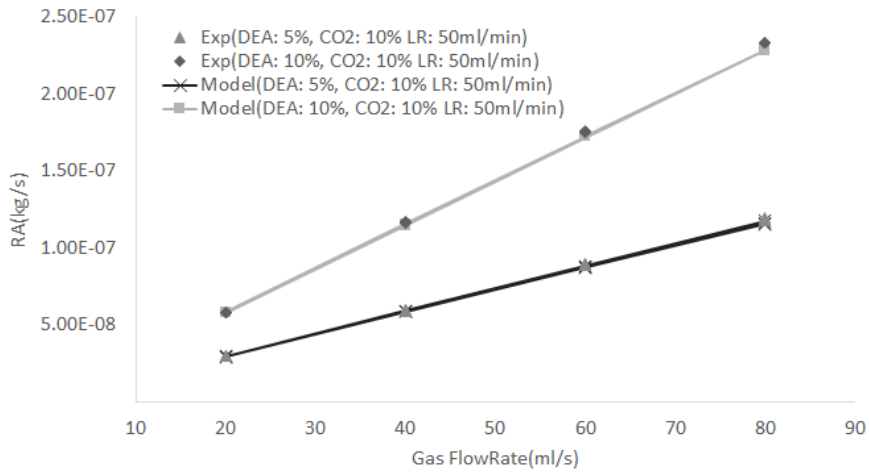
Fig. 9 – comparison of CO_2 absorption rate using DEA by model and the result from setup.

The effect of various operational parameter on the absorption process is simulated with COMSOL Multiphysics. Figure 8 shows the concentration variation of CO_2 in the gas phase for FFR (Amine flowrate: $8.33 \times 10^{-7} m^3/s$, CO_2 concentration at the input gas: 10%, DEA aqueous solution Concentration: 25%). It has been observed that most of the CO_2 absorption and mass transfer occurred in a short section of FFR. When the gas flow rate has changed from 3.33×10^{-7} to $1.33 \times 10^{-6} (m^3/s)$, the output concentration increased. As the gas flow rate increased, the gas velocity increased and the resident time decreased, so the CO_2 moles had less time to react with DEA.

The simulation shows that the temperature of the falling film has been approached to the cooling water temperature very soon because the falling film thickness was very thin (approximately 0.2mm), and close agreement between simulation results and experimental data is observed (Figure 9).

2. RSHM & CO_2 absorption using DEA in FFR

Design expert can be used to model many chemical processes and is an effective tool in experimental design.[29,30] The variables studied in this work are DEA (wt%) (A), gas flow rate (mL/min) (B), DEA flowrate (mL/min) (C) and input CO_2 concentration (ppm) (D), to determine absorption rate or gain (R_A (kg/s)). The range of these parameters was selected based on laminar flow in the liquid phase, gas phase ($1 \leq Re_G \leq 6$ and $4 \leq Re_L \leq 40$ at 298 K) and setup specification. 2FI(two-factor interactions) model is used to determine response(R_A) according to effective factors(A, B, C, D) on the absorption process.

2.1. 2FI Model and ANOVA Analysis

The experimental data were analyzed and a 2FI model was developed to correlate process parameters with the response, as presented in the following equation in terms of coded factors.

$$R_A = 1.068E\text{-}7 + 1.156E\text{-}9A + 6.266E\text{-}8B - 1.686E\text{-}9C + 4.055E\text{-}8D + 9.13E\text{-}10AB + 4.201E\text{-}10AC + 5.585E\text{-}10AD - 1.978E\text{-}9BC + 2.416E\text{-}8BD - 9.026E\text{-}10CD \qquad (17)$$

In the linear terms, A, B, D and in the interaction terms, AB, AC, AD, and BD have a significant synergistic effect on the response, since they have a positive coefficient, whereas the negative coefficient of C, BC and CD show a significant antagonistic effect.
The model has an F-value of 18391.39 (much greater than unity) and a p-value of 0.0001 (<0.05), which also implies that the model is significant. There is only a 0.01% chance that an F-value this large could occur due to noise. In this case, A, B,

C, D, AB, AC, AD, BC, BD, CD are significant model terms. The R^2 value for the 2FI model is 0.9997. The "Pred R-Squared" of 0.9995 is in reasonable agreement with the "Adj R-Squared" of 0.9997, expressing that the model is significant. An adequate precision value of 440.864 (>4) implies an adequate signal ratio. So this model can be used to navigate design space.

Normal Plot of Residuals is shown in Figure 10 and it is observed that the values on this graph are very close to red lines and this is due to a low error.
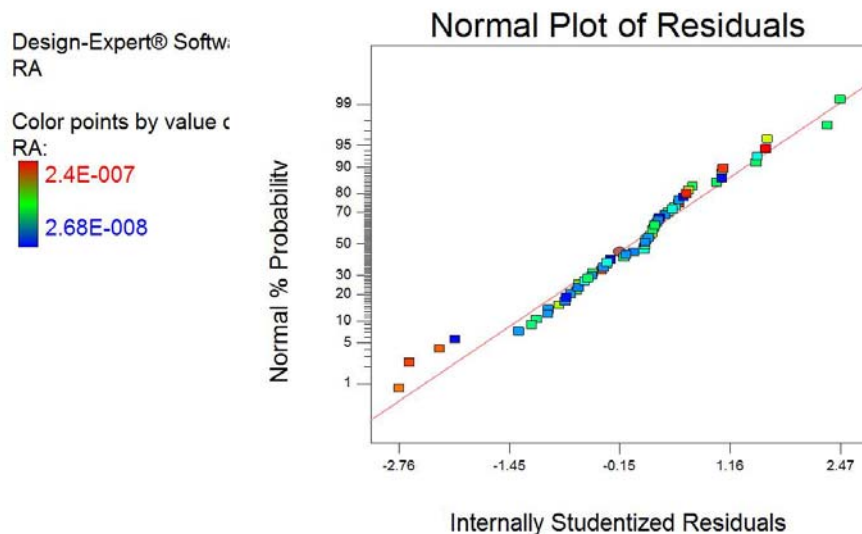
Fig. 10 – Normal Plot of Residuals for Eq. 7.
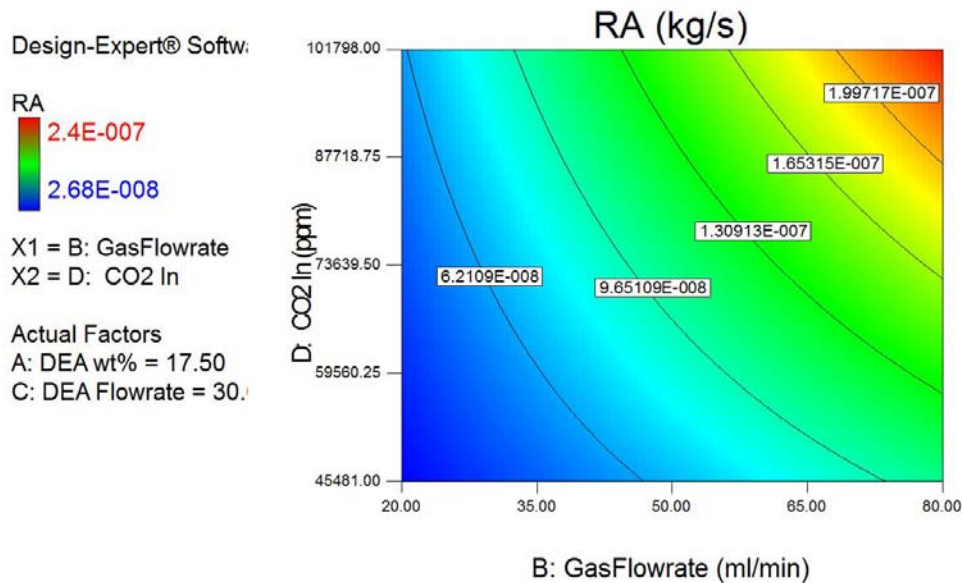
Fig. 11 – Contour plot for CO_2 absorption(R_A(kg/s) as a function of gas flow rate(mL/min)
and CO_2 input ppm at a DEA % of 17.5 and a DEA flowrate of 30 mL/min.

2.2. Response surface analysis

To understand the behavior of various process variables, Contour plots were generated. The effect of two parameters, keeping the third and fourth constant, is depicted in Figure 11. It is observed that when DEA percent and DEA flowrate were constant, an increase in CO_2 input concentration and gas flow rate has been increased the absorption rate. At a fixed gas flow rate, the CO_2 absorption rate was a strong function of CO_2 input ppm.

CONCLUSIONS

DEA can be used to reduce the CO_2 concentration from the flue gas. Falling film reactor is a very useful tool for this purpose and operating parameter could be controlled to get optimum result. The numerical modeling of the CO_2 absorption process in FFR is simulated by COMSOL Multi-physics software environment 5.1 and a clear picture of the reaction occurred in the reactor is shown. The model has predicted the setup data precisely. The penetration depth of CO_2 into the falling film of DEA was 0.006 mm. Since most of the CO_2 absorption and mass transfer occurred in a short section of FFR, it is suggested that the size of the reactor could be reduced.

In a falling film reactor, 2FI model can be used to predict the absorption rate of CO_2 in terms of the operating parameters, and for low Reynolds number, gas flowrate and CO_2 input concentration can be the most effective parameters.

Nomenclature

A   gaseous reactant
a_c correction factor for the interfacial area, $(d - 2\delta)/d$
B   liquid reactant
C_A concentration of dissolved gas A (kmol/m^3)
C_{AG} concentration of A in bulk gas (kmol/m^3)
C_B concentration of Reactant B (kmol/m^3)
C_B^O inlet concentration of Reactant B (kmol/m^3)
d   inner diameter of the column (m)
D_G diffusion coefficient of CO_2 in gas (m^2/s)
H_o Henry's constant
h_G heat transfer coefficient in gas phase (J/s m^2 K)
k   second order rate constant at a temperature T_r (m^3/kmol s)
k_G mass transfer coefficient (m/s)
k_λ thermal conductivity (W/m K)
L   height of the column (m)
Q_L volumetric flow rate of liquid (m^3/s)
Q_G volumetric flow rate of gas (m^3/s)
r   rate of reaction (kmol/m^{3}s)
R_A rate of absorption (kg/s)
Re_G gas-phase Reynolds number, $(d - 2\delta)\, u_G\rho_G/\mu_G$
Re_L liquid-phase Reynolds number, $4\Gamma/\mu_L$
Sc_G Schmidt number, $\mu_G/\rho_G D_G$
Sh_G Sherwood number, $k_G a_c d/D_G$
T   liquid temperature (K)
T_G gas-phase temperature (K)

T_o inlet liquid temperature (K)
T_R temperature of cooling water (K)
U overall heat transfer coefficient for cooling water (J/s m^2 K)
u_G velocity of gas film (m/s)
u_L axial velocity of liquid film (m/s)
w_G molar flow rate of gas per unit wetted perimeter (kmol/(m s))
x radial coordinate (m)
z axial coordinate (m)
$-\Delta H_R$ Heat of reaction (J/kmol)
$-\Delta H_S$ Heat of solution (J/kmol)

Greek letters
Γ volumetric liquid flow rate (m^3/s)
δ liquid film thickness (m)
μ liquid viscosity (kg/m s)
ν kinematic viscosity of liquid (m^2/s)
ρ liquid density (kg/m^3)
τ shear stress (N/m^2)
α thermal diffusivity (m^2/s)

Subscripts
G   gas phase
i   interface
in   inlet
L   liquid phase
out   outlet

REFERENCES

1. Y. Gao, X. Gao and X. Zhang, *Engineering*, **2017**, *3*, 272–278.
2. M. M. Ghiasi and A. H. Mohammadi, *J. Nat. G. Sci. Eng.*, **2014**, *18*, 39–46.
3. I. P. Koronaki, L. Prentza and V. Papaefthimiou, *Renewable and Sustainable Energy Reviews.*, **2015**, *50*, 547–566.
4. Akanksha, K. K. Pant and V. K. Srivastava, *Chem. Eng. J.*, **2007**, *133*, 229–237.
5. V. V. Chavan and R. A. Mashelkarr, *Chem. Eng.*, J., **1972**, *4*, 223–228.
6. Frederic K. Wasden and A. E. Dukler, *AIChE J.*, **1990**, *36*, 9–14.
7. T. Conlisk, *AIChE J.*, **1992**, *38*, 11–16.
8. R. Yang and D. Jou, *Can. J. Chem. Eng.*, **1993**, *71*, 533–538.
9. G. M. Sisoev, O. K. Matar and C. J. Lawrence, *Chem. Eng. Sci.*, **2005**, *60*, 827–838.
10. J. Hu, X. Yang, J. Yu and G. Dai, *Chem Eng Sci.*, **2014**, *116*, 243–253.
11. H. Pedersen and J. E. Prenosil, *Int. J. H. M. Tran.*, **1981**, *24*, 299–304.
12. M. Danish, R. K. Sharma and S. Ali, *App. Math. Mod.*, **2008**, *32*, 901–929.
13. P. Moschou, M. H. J. M. de Croon, J. van der Schaaf and J. C. Schouten, *Chem. Eng. Sci.*, **2012**, *76*, 216–223.
14. A. Servia, N. Laloue, J. Grandjean, S. Rode and C. Roizard, *O. & G. Sci. Tech.*, **2014**, *69*, 5–10.
15. S. A. Gheni, M. F. Abed, E. K. Halabia and S. R. Ahmed, *O & G Sci. Tech.*, **2018**, *73*, 43–48.
16. W. G. Whitman, *Int. J. H. M. Tran.*, **1962**, *5*, 429–433.
17. C. Wang, Z. Xu, C. Lai and X. Sun, **2018**, *184*, 103–110.
18. F. Zhang L. Guo, Y. Ding, X. Zhu and Q. Liao, *Appl. Therm. Eng.*, **2018***, 138*, 583–590.
19. V. Russo, A. Milicia, M. Di Serio and T. Riccardo, *Chem. Eng. J.*, **2019,** *377*, 120464–120470.
20. W. Kaewboonsong, V. I. Kuprianov and N. Chovichien, *F. Proc. Tech.*, **2006**, *87*, 1085–1094.
21. U. S. P. R. Arachchige, N. Aryal, D. A. Eimer and M. C. Melaaen, *Ann. Transact. N. R. Soc.*, **2013**, *21*, 229–306.
22. J. Han, J. Jin, D. A. Eimer and M. C. Melaaen, *J. Chem. Eng. Data.*, **2012**, *57*, 1843−1850.
23. M. Shokouhi, A. H. Jalili and M. Hosseini-Jenab, *IAChE,* **2013,** *10*, 43–54.
24. E. D. Snijder, M. J. M. Riele, G. F. Versteeg and W. P. M. van Swaaij, *J. Chem. Eng.,* **1993**, *3*, 475–480.
25. M. K. Abu-Arabi, A. M. Al-Jarrah, M. El-Eideh and A. Tamimi, *J. Chem. Eng. Data.,* **2001**, *46*, 516–521.
26. Y. E. Kim, J. A. Lim, S. K. Jeong, Y. I. Yoon, S. T. Bae and S. C. Nam, *B. Kor. Chem. Soc.*, **2013**, *34*, 783–787.
27. H. Kierzkowska-Pawlak and A. Chacuk, *J. A. & W. Man. Assoc.*, **2010**, *60*, 925–931.
28. D. Sebastia-Saez, S. Gu, P. Ranganathan and K. Papadikis, *Inter. J. G. Gas Con.*, **2015**, *33*, 40–50.
29. M. Kokare, B. Manali, V. Ranjani and C. S. Mathpati, *Chem. Eng. Re. and De.*, **2018**, *137*, 577–588.
30. D. M. K. Nguyen, T. Imai, T. L. T Dang, A. Kanno, T. Higuchi, K. Yamamoto and M. Sekine, *J. Environ. Sc*i., **2017**, *65,* 116–126.